Behavior and Design of Link Slabs for Jointless Bridge Decks

Alp Caner, Ph.D.
Structural Engineer
Parsons Brinckerhoff Quade and Douglas
New York, New York

Paul Zia, Ph.D., P.E.
Distinguished University Professor of Civil Engineering (Emeritus)
North Carolina State University
Raleigh, North Carolina

Maintenance of bridge deck joints is a costly problem. Debris accumulation in the joints can restrain deck expansion, causing undesirable forces in the deck and damage to the structure. Water leaking through the joints is a major cause for the deterioration of bridge girder bearings and supporting structures. Therefore, elimination of deck joints at the supports of multispan bridges will reduce the cost of construction and maintenance. This paper presents the results of a test program to investigate the behavior of link slabs connecting two adjacent simple-span girders, and proposes a simple method for designing the link slab. To illustrate the proposed design method, three design examples are included.

Many highway bridges are designed as multiple simple-span composite structures that utilize either steel or prestressed concrete girders and a cast-in-place concrete deck spanning from one pier (or bent) to another. At each end of the simple-span deck, a joint is provided for deck movement due to temperature, shrinkage, and creep effects.

Bridge deck joints are a persistent and costly maintenance problem. Water leaking through the joints is a major cause for the deterioration of bridge girder bearings and supporting structures. Debris accumulation in the joints restrains deck expansion and causes damage to the bridge. Joints and bearings are expensive to install and maintain. Therefore, the cost of construction and maintenance for a bridge can be greatly reduced if the number of deck joints in multi-span bridges can be minimized.

It should be noted that when the deck joints are removed and replaced by a jointless deck, fine cracks can be expected to develop in the jointless deck and in many cases water may still leak through the fine cracks. However, the situation is preferable to that of jointed decks.

During the last several years, bridge engineers have designed different types of jointless bridge decks. Integral bridges are jointless and designed as single- or multiple-span continuous bridges with capped pile-stub type abutments. Burke[1-3] has discussed the attributes and limitations of integral bridges. The use of prestressed concrete piles in integral abutment

bridges has been discussed by Kamel et al.[4]

Jointless bridge decks with continuous girders are commonly used in many states. Wasserman[5] and Loveall[6] have described their extensive experience with such bridges in Tennessee. Their experience included both bridge rehabilitation and new construction.

A comprehensive study of jointless decks with continuous girders was conducted by Oesterle et al.[7] In their study, the precast, prestressed girders were made continuous to resist live load by the use of continuity steel and end diaphragms at the bridge piers. Their design recommendations have been used by many state highway departments; however, the required deck reinforcement tends to be excessive. In actual practice, most bridge engineers have used a smaller amount of reinforcing steel based on their own judgment and experience. In addition, the end diaphragm is a difficult construction detail to execute in the field.

Bridge deck joints can also be eliminated by making the deck continuous while keeping the girders as simple-spans. The section of the deck connecting the two adjacent simple-span girders is called the link slab.[8]

Jointless bridge decks supported by simple-span girders have been used both in the United States and abroad.[9-11] Two such examples are shown in Fig. 1. It is noted that end diaphragms separated by two layers of smooth roofing paper are used by the Florida DOT but no diaphragms are used by the Texas DOT. By eliminating the end diaphragms, this construction detail is greatly simplified.

In 1981, Zuk[12] studied the concept of jointless bridge decks built on multiple simply-supported girders. He analyzed the effects of expansion and contraction of the jointless deck and considered the interactive forces between the girders and the deck. Although the concept seemed promising, it was not used in any actual applications.

In the late 1980s, Gastal and Zia[13] described the results of a finite element method of analysis for jointless bridge decks supported by simple-span girders. The analysis accounted for the nonlinear material properties, cracking of concrete, creep, shrinkage,

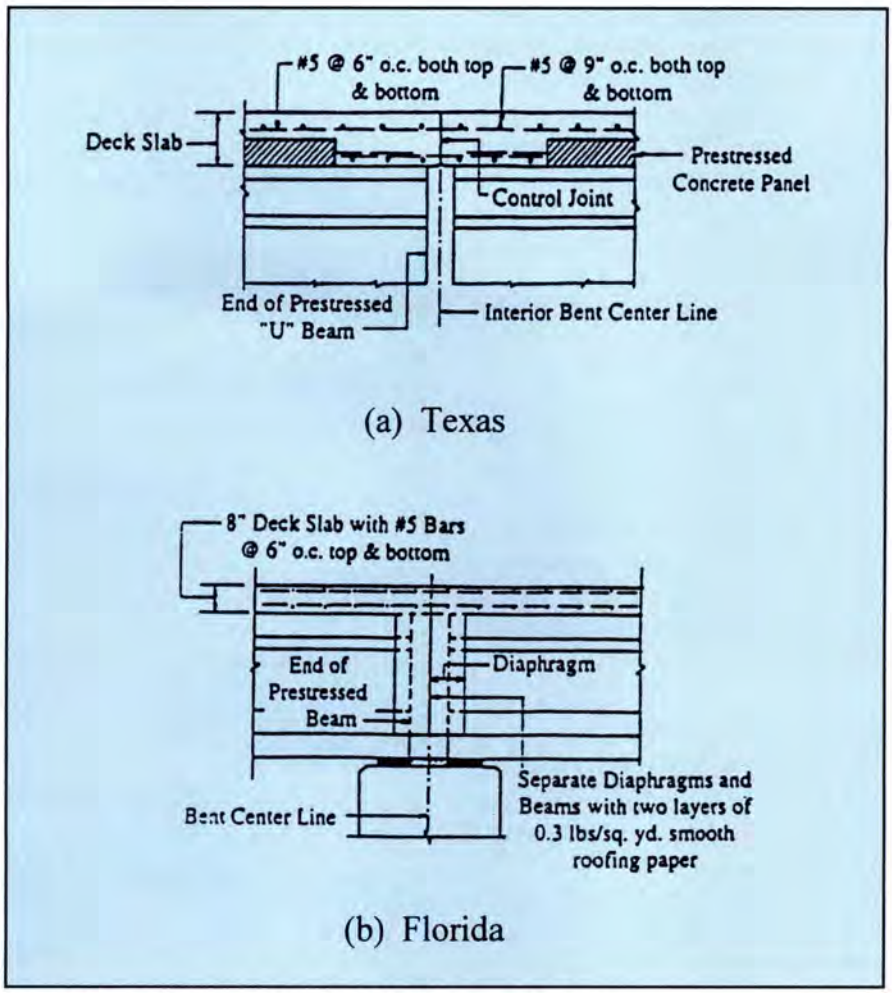

Fig. 1. Typical jointless bridge deck. **Note:** 1 in. = 25.4 mm; 1 lb per sq yd = 0.543 kg/m^2.

temperature effects and various loading conditions. For lack of experimental data, the computer solutions were validated by comparisons with the results of several different tests of simply-supported beams (without a jointless bridge deck) that were reported in the literature.

El-Safty[8] modified Gastal's finite element program[14] by incorporating an optional analysis for partial debonding of the deck from the supporting beams. He also introduced the assumption of constant strain through the depth of the link slab, whereas Gastal assumed a linearly varying strain through the depth of the link slab.

Richardson[15] also studied the removal of expansion joints from bridges using continuous and partially debonded decks and developed a simplified design procedure. Computer programs were developed to predict the crack width and spacing in the deck and to calculate the vertical deflection of the structure.

These analytical studies notwithstanding, no experimental validation of the concepts of analysis and design for jointless bridge decks supported by simple-span girders can be found in the literature. This paper presents the results of a test program to investigate the behavior of the jointless bridge deck, and proposes a simple design method for the link slab.[16,17] Three numerical design examples are included to demonstrate the proposed design method.

TEST PROGRAM

The test program included two large test specimens of composite construction, one being a continuous reinforced concrete deck slab cast on two simple-span steel beams, and the other being a similar slab cast on two simple-span precast reinforced concrete

beams. Fig. 2 shows the details of the two test specimens. The material and geometrical properties of both specimens are given in Table 1. Fig. 3 shows a general view of the test setup for the concrete bridge under the ultimate load test. Detailed descriptions of instrumentation can be found in Refs. 16 and 17.

It should be noted that even though this test program used steel and precast reinforced concrete beams, the concept being evaluated should be directly applicable to bridge deck rehabilitation with existing precast, prestressed concrete girders. The concept is also applicable to new bridge construction using precast, prestressed concrete girders if the effects of creep and shrinkage are adequately accounted for.

Steel Bridge

The first specimen represented a steel bridge with a jointless composite concrete deck. Two simply-supported W12x26 steel beams, each 20.5 ft (6.25 m) long, were aligned with a 2 in. (50.8 mm) gap between the adjacent ends of the two beams. These two steel beams were then joined with a continuous concrete deck reinforced with three #6 epoxy coated longitudinal bars, thus creating a 41 ft 2 in. (12.55 m) long two-span structure with a jointless deck supported by two simple-span beams (see Fig. 2). A row of 0.75 in. (19 mm) shear connectors spaced at 17 in. (432 mm) were welded to the top of the steel beams to develop composite action with the reinforced concrete deck, except in the deck debonded zone as described below.

The concrete deck was 2 ft (610 mm) wide, 4 in. (102 mm) thick, and 41 ft 2 in. (12.55 m) long. At the two adjacent ends of the steel beams, the concrete deck was debonded from each steel beam for a distance of 12 in. (305 mm), which was 5 percent of the span of each beam. The 5 percent debonding length was based on the results of theoretical studies that showed that the load-deflection behavior of the structure would not be affected by a debonding length of up to 5 percent of the span length.[8] The purpose of debonding is to reduce the stiffness of

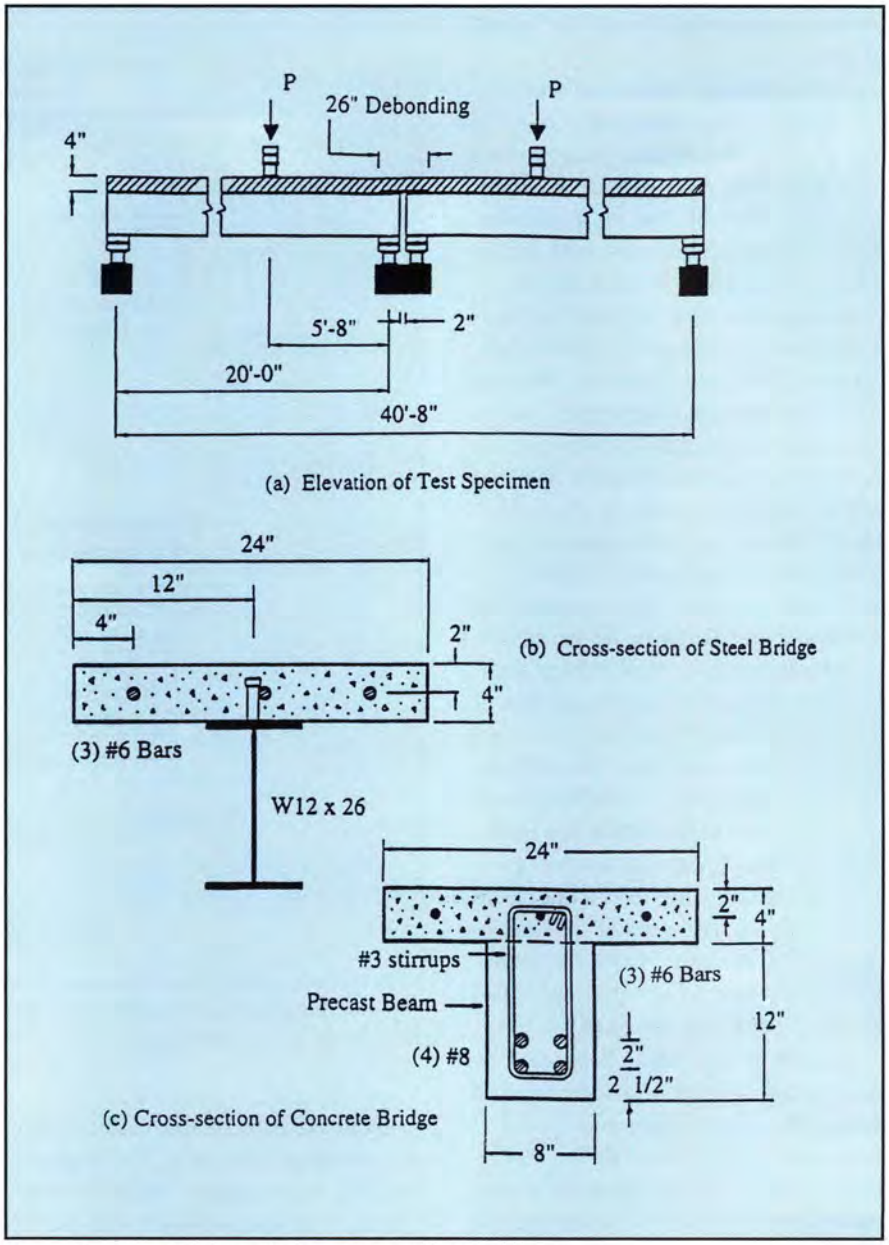

Fig. 2. Details of test specimens. **Note:** 1 in. = 25.4 mm.

Table 1. Material and geometrical properties of steel and concrete bridges.

Properties	Steel bridge	Concrete bridge
Compressive strength of concrete deck	4200 psi	5670 psi
Compressive strength of girder	—	4580 psi
Girder yield strength	52,000 psi	—
Girder modulus of elasticity	30,500,000 psi	—
Girder reinforcement	—	(4) #8
Girder reinforcement yield strength	—	62,000 psi
Girder reinforcement modulus of elasticity	—	29,550,000 psi
Girder cross-sectional area (gross)	7.65 sq in.	96 sq in.
Girder moment of inertia (gross)	204 in.^{4}	1152 in.^{4}
Deck width	24 in.	24 in.
Deck thickness	4 in.	4 in.
Link slab reinforcement	(3) #6	(3) #6
Link slab reinforcement yield strength	63,600 psi	72,400 psi
Link slab reinforcement modulus of elasticity	28,500,000 psi	30,300,000 psi

Note: 1 in. = 25.4 mm; 1 sq in. = 645.2 mm^2; 1 psi = 0.006895 MPa.

the link slab so that the stress developed in the link slab can be minimized.

The continuity of the deck reinforcement in the debonding zone was developed by a lap splice 17 in. (432 mm) long to simulate the situation where a damaged joint of a bridge deck would be removed and replaced by a jointless deck. The computed moment capacity of the composite section was 247 ft-kips (335 kN-m), based on the actual material properties given in Table 1.

Concrete Bridge

The second specimen represented a concrete bridge with a jointless deck. First, two 20.5 ft (6.25 m) long reinforced concrete beams were precast in the laboratory. The beams were 12 in. (305 mm) high and 8 in. (203 mm) wide. Each beam was reinforced with four #8 bars and thirty-one #3 stirrups. A deck of the same size as that of the first specimen was cast on the precast beams when the concrete of the beams had gained enough strength.

As before, the jointless deck was also debonded from each beam for a distance of 12 in. (305 mm) at the center of the specimen. Debonding was achieved by omitting the stirrups and by placing two layers of plastic sheet between the beam and the deck. The longitudinal reinforcement in the deck consisted of three #4 bars which, in turn, were lap spliced with three #6 epoxy coated bars at the center of the specimen. The computed moment capacity of the composite section was 185 ft-kips (251 kN-m), based on the actual material properties given in Table 1.

TEST PROCEDURE

The test procedure used for both specimens was similar. The steel bridge was tested with four different support configurations: HRRH, RHRH, RRRR and RHHR, where H stands for hinge and R stands for roller. In each configuration, the first and fourth letters represent the two exterior supports. The second and third letters represent the two interior supports. A hinge was provided by using a 1.5 in. (38 mm) diameter steel pin between two 1.5 in. (38 mm) thick bearing plates, each with a V-groove. A roller was provided by using the same size pin and plates but without V-grooves.

Fig. 3. Concrete bridge during ultimate load test.

The concrete bridge was tested with the same support conditions, except for the RRRR configuration, which is an unlikely support condition in the field. The goal in testing different support conditions was to observe if there were any differences in the behavior of the jointless deck (i.e., link slab) under different support conditions, as previously predicted by El-Safty's computer model.[8]

In all cases, tests were carried out to no more than 40 percent of the estimated ultimate load capacity of each test specimen to observe the behavior in the elastic range. The load P was applied on each span in increments. For each load increment, data for the steel and concrete strains, loads, crack growth and deflections were collected. The final ultimate load test was performed with the support configuration of RHHR and a complete set of data on strains, loads, crack widths, and deflections was collected.

TEST RESULTS

A discussion of the test results will be given first for the steel bridge and then for the concrete bridge.

Steel Bridge

The steel bridge was tested with four different support configurations, namely, HRRH, RHRH, RRRR, and RHHR. Initially, the load was applied up to 17.4 kips (77.4 kN) on each span to observe the behavior in the elastic range. Within this elastic range, the load-deflection behavior was comparable for all the four test cases, as shown by the measured load-deflection relationships in Table 2. In addition, the load-deflection behavior was almost identical for both spans of the test specimen as required by symmetry.

It is noted that the measured slopes of the load-deflection curves are comparable to the theoretical value. The theoretical value is obtained by using the average of the moment of inertia of a fully composite section and the moment of inertia of the steel beam

Table 2. Slope of load-deflection curve (kips/in.).

Support configuration	Steel bridge		Concrete bridge	
	Experimental	Theoretical	Experimental	Theoretical
HRRH	55.8	52.6	57.6	52.3
RHRH	58.7	52.6	55.0	52.3
RRRR	49.6	52.6	—	—
RHHR	54.8	52.6	54.8	52.3

Note: 1 kip/in. = 0.175 kN/mm.

alone. This approach is justified to account for the effect of slip between the deck and the steel beam, except at the locations of the studs. Therefore, the stiffness of the composite beam is less than that of a fully composite section due to the incomplete interaction between the deck and the steel beam.[18]

The measured deflections also compared closely with the predicted deflections, using El-Safty's structural analysis program,[8] by neglecting the link slab and treating the bridge as two simply-supported spans. It indicates that the behavior of the steel bridge with a jointless deck was similar to a simply-supported bridge.

The strains in the two steel beams measured at 13 ft (4.01 m) from the exterior supports were similar in all four test cases. Both spans of the bridge had almost the same strain variations under the test load. These measurements indicated tension in the bottom flange and a small amount of compression in the top flange of the steel beam. The strain variation along the depth of the steel section was virtually linear. Under the applied load of 17.4 kips (77.4 kN), the tensile stress in the bottom flange was 17.6 ksi (121.4 MPa), which was only one-third of the yield strength of the steel.

The tensile strains developed in the #6 epoxy coated bars in the link slab were again similar for all four of the test cases. Under the first increment of loading, a fine crack was developed that passed through the center of the link slab where the strain gauges on the reinforcement were located. At the load level of 17.4 kips (77.4 kN), the tensile stress in the link slab reinforcement was about 30 percent of its yield strength.

The five strains measured by the Demec gauges on the top surface of the link slab were comparable in magnitude at each load level. The strains measured by the Demec gauges on the side faces of the link slab showed that the bottom portion of the deck was in compression. It was also observed that the crack at the center of the link slab did not extend to the bottom face of the slab. Thus, the link slab was in bending and behaved like a beam rather than a tension member.

For the ultimate load test, the load-deflection curve was linear up to the load level of 30 kips (133.4 kN) when the steel beams began to yield. When the load reached 42.9 kips (190.8 kN), the deflectometers were removed because the beam deflection was about to exceed the range of the deflectometer. The maximum load capacity was reached at 45 kips (200.2 kN).

In the ultimate load test, the stress in the bottom flange of the steel beam reached the yield strength of 52 ksi (358.5 MPa) under an applied load of 30 kips (133.4 kN). When the load was increased to 42.9 kips (190.8 kN), the entire bottom flange and roughly two-thirds of the web of the steel beam exceeded the yielding strain of the steel beam, which was 1705 micro-strains.

Failure was initiated by yielding of the steel beam at a load level of 30 kips (133.4 kN), followed by yielding of the reinforcing bars in tension in the link slab at a load of 39.8 kips (177 kN). The link slab cracked at five different locations. When the load reached 45 kips (200.2 kN), crushing of concrete was observed at the bottom portion of the link slab, indicating final failure of the link slab.

The crack widths were measured on the top surface of the link slab during the ultimate load test. A total of five cracks were observed. Two of the cracks were developed in the previous tests for elastic behavior and the remaining three cracks were developed during the ultimate load test.

The crack at the center of the link slab had the largest crack width. Along this crack, its width was measured at five points 4 in. (102 mm) apart. The growth of the average crack width for this crack was from 0.012 in. (0.30 mm) at 40 percent of the ultimate load to 0.029 in. (0.74 mm) at 67 percent of the ultimate load when the bottom fibers of the steel beam began to yield, and finally to 0.24 in. (6.1 mm) at the ultimate load. At these three load levels, the corresponding stress in the link slab reinforcing bar was 19.1, 30.4 and 63.6 ksi (132, 210 and 439 MPa), respectively.

Concrete Bridge

The concrete bridge was tested for three different support configurations: HRRH, RHRH and RHHR. In each case, the load was applied up to 16 kips (71.2 kN) and the specimen remained in the elastic range. Within this range, the load-deflection behavior was practically the same for the three test cases, as shown by the slopes of the load-deflection relationships given in Table 2. In addition, the load-deflection behavior was almost identical for both spans of the test specimen, as required by symmetry.

As in the case of the steel bridge, the behavior of the concrete bridge with a jointless deck was similar to a simply-supported bridge rather than a partially continuous bridge. Furthermore, the stiffness of the concrete bridge was almost the same as that of the steel bridge (see Table 2).

The strains in the reinforcing bars were measured at 14 ft (4.27 m) from the exterior supports for all four bars in the right-hand span and for only one bar in the left-hand span. These measured strains were similar in all three tests for loads below 40 percent of the ultimate load. At a load of 16 kips (71.2 kN), the tensile stresses in the bars at the top and bottom layers were 16.8 and 20.8 ksi (116 and 143 MPa), respectively.

The tensile strains developed in the #6 epoxy coated bars in the link slab were again similar for the three test cases. Throughout the tests, bending of the link slab was observed just as that which occurred in the steel bridge. Two visible cracks developed at the center of the link slab. At the load of 16 kips (71.2 kN), the tensile stress developed in the link slab reinforcement was 18.6 ksi (128.2 MPa).

In the ultimate load test, measured deflections were small for loads up to 33.8 kips (150.3 kN). When the load reached 33.8 kips (150.3 kN), yielding of the four #8 bars in each of the concrete beams occurred. At a load level of 36 kips (160.1 kN), major shear cracks developed in both spans. With a load of 37.5 kips (166.8 kN), the reinforcement in the link slab reached its yield strength.

When the load reached 38.7 kips (172.1 kN), the deflectometers were removed from below the beams because of excessive deformations. The maximum load carrying capacity was

reached at 43 kips (191.3 kN) when the right-hand span failed first with the crushing of the concrete deck in the compression zone near the load point. At the same time, the bottom portion of the link slab also failed due to concrete crushing.

The crack widths were measured on the top surface of the link slab in all test cases, including the elastic and ultimate load tests. The measurements were similar in all cases. Two cracks were observed during the tests. At 37 percent of the ultimate load, the average width of the two cracks was 0.010 in. (0.254 mm). It increased to 0.024 in. (0.61 mm) at 78 percent of the ultimate load when the reinforcing bars in the beam began to yield, and then to 0.038 in. (0.97 mm) at 90 percent of the ultimate load. At these three load levels, the corresponding bar stress in the link slab was 18.6, 40.2 and 56.5 ksi (128, 277 and 390 MPa), respectively. At the ultimate load, the crack width exceeded the maximum scale of the crack comparator card, which was 0.060 in. (1.50 mm).

ANALYTICAL STUDIES

This section shows how the service load was calculated, presents the simplified method of analysis, and outlines the structural computer program for solving the link slab problem in both a steel bridge and a concrete bridge.

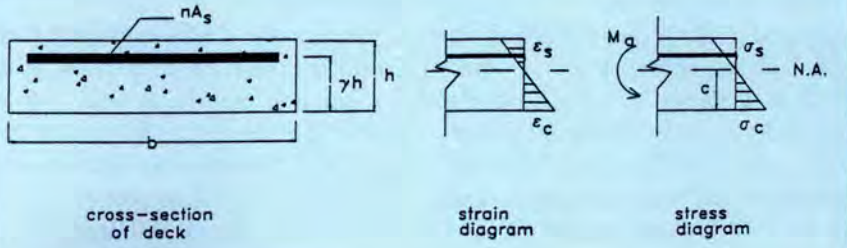

Ratio of tension reinforcement:

$$\rho = (A_s / b\gamma h) \quad (1)$$

Area of tension reinforcement:

$$A_s = \rho\gamma bh \quad (2)$$

From moment equilibrium:

$$M_a = A_s\sigma_s(\gamma h - c/3) = \rho\gamma bh\sigma_s(\gamma h - c/3) \quad (3)$$

The depth of compression zone, c, can be determined from:

$$0.5bc^2 = n\rho\gamma bh(\gamma h - c) \quad (4)$$

where n is the modular ratio of steel to concrete.
From Eq. (4), c will be:

$$c = -n\rho\gamma h + \gamma h[(n\rho)^2 + 2n\rho]^{0.5} \quad (5)$$

The moment of inertia of the cracked section can be expressed as:

$$I_{cr} = (0.333)bc^3 + nA_s(\gamma h - c)^2 \quad (6)$$

The cracking moment will be:

$$M_{cr} = (f_r I_g)/y = (f_r bh^2)/6 \quad (7)$$

where f_r is the flexural tensile strength of the concrete.
The ratio of M_{cr} to M_a will be:

$$M_{cr}/M_a = f_r/(6f_s\rho\gamma^2\{1 + n\rho/3 - 0.333[(n\rho)^2 + 2n\rho]^{0.5}\}) \quad (8)$$

The stress in reinforcement will be:

$$f_s = f_r M_a/(6M_{cr}\rho\gamma^2\{1 + n\rho/3 - 0.333[(n\rho)^2 + 2n\rho]^{0.5}\}) \quad (9)$$

Fig. 4. Internal bending stresses and strains in link slab.

Calculation of Service Load

The service load for each test specimen is determined according to the AASHTO Specifications.[14] The required moment capacity M_u of a girder is related to its dead load moment M_d and live load moment M_l plus impact through the load factors:

$$M_u = 1.3\ (1.0M_d + 1.67M_{l+i})$$

The design strength of a girder is equal to its nominal moment capacity M_n multiplied by the capacity reduction factor ϕ, and the design strength must be equal to or larger than the required moment capacity. From a review of three typical NCDOT bridge girders, it was found that the ratio of dead load moment to live load moment plus impact is roughly 0.53.

Therefore:

$$\phi M_n = M_u = 1.3(0.53M_{l+i} + 1.67M_{l+i}) = 1.3(2.20M_{l+i}) = 2.86M_{l+i}$$

$$M_n = (M_u/\phi) = 2.86M_{l+i}/0.9 = 3.18M_{l+i}$$

Because the nominal moment capacities of the steel and concrete bridges are 247 and 185 ft-kips (335 and 251 kN-m), respectively, the service live load moment plus impact would be 77.7 ft-kips (104.8 kN-m) for the steel bridge and 58.2 ft-kips (78.8 kN-m) for the concrete bridge.

If the two test specimens were treated as simply-supported members by neglecting the effect of the link slab, the concentrated load required to produce the above service moments at the critical section (i.e., load point) would be 19.1 kips (84.9 kN) (64 percent of the elastic limit) for the steel bridge and 14.3 kips (63.6 kN) (42 percent of elastic limit) for the concrete bridge, respectively. These concentrated loads indicate that under service moment condition, the beams would behave well within their elastic ranges, and the loads also compare reasonably well with the test loads of 17.4 kips (77.4 kN) for the steel bridge and 16 kips (71.2 kN) for the concrete bridge, respectively, to observe their elastic behavior.

Simplified Method of Analysis

Because the stiffness of the link slab is much smaller than the stiffness of the girders, the link slab introduces a negligible amount of continuity to the

structure. Therefore, each span of the bridge can be treated as a simply-supported girder and its deflection can be calculated by neglecting the effect of the link slab. Under live load, the end rotations of two adjacent girders will cause bending of the link slab. Therefore, the link slab can be analyzed as a beam subjected to the same end rotations as the adjacent girders. These imposed end rotations induce a moment in the link slab.

To determine this induced moment, the section properties (area and moment of inertia) of the link slab must be obtained first. During the tests, it was observed that most cracks developed in the center portion of the link slab and only a few small cracks developed in the debonded portions of the link slab.

To account for the stiffness variation, the section properties of the center portion of the link slab are calculated based on a cracked section, and the section properties of the two outer debonded portions of the link slab are obtained using the averages of the gross and cracked section properties. The equations developed for computing the moment of inertia of a cracked section and the steel stress in the link slab are summarized in Fig. 4.

The crack width at the surface of the central portion of the link slab can be estimated using the crack criteria given in the AASHTO Specifications,[19] which is based on the Gergely-Lutz[20] expression:

$$\omega = 0.076\beta f_s (d_c A)^{1/3}$$

where

ω = surface crack width in units of 0.001 in. (0.03 mm)
β = ratio of distances to neutral axis from extreme tension fiber and from centroid of main reinforcement
f_s = reinforcement stress in ksi (MPa)
d_c = concrete cover measured from extreme tension fiber to centroid of nearest reinforcement level in in. (mm)
A = effective area per bar in sq in. (mm^2)

Table 3a. Comparison of test results with predictions by JBDS program for steel bridge with HRRH support configuration.

Results	Applied load P (kips)	Midspan deflection		Exterior reaction (kips)	Interior reaction (kips)	Strain at bottom flange	
		East (in.)	West (in.)			East μ (in./in.)	West μ (in./in.)
Test	3.37	0.04	0.04	0.73	2.64	71	93
JBDS	3.37	0.04	0.04	0.95	2.41	103	103
Test	7.15	0.10	0.10	1.75	5.40	188	219
JBDS	7.15	0.10	0.10	2.03	5.13	218	218
Test	11.80	0.18	0.18	3.00	8.80	334	363
JBDS	11.80	0.16	0.16	3.34	8.46	359	359
Test	15.34	0.25	0.25	4.05	11.29	474	483
JBDS	15.34	0.20	0.20	4.34	11.00	467	467
Test	17.43	0.31	0.31	4.94	12.49	619	596
JBDS	17.43	0.23	0.23	4.94	12.29	531	531

Note: 1 in. = 25.4 mm; 1 kip = 4.45 kN.

Table 3b. Comparison of test results with predictions by JBDS program for concrete bridge with HRRH support configuration.

Results	Applied load P (kips)	Midspan deflection		Exterior reaction (kips)	Interior reaction (kips)	Strains in reinforcing bar at bottom of beam	
		East (in.)	West (in.)			East μ (in./in.)	West μ (in./in.)
Test	2.11	0.03	0.03	0.55	1.56	71	—
JBDS	2.11	0.02	0.02	0.60	1.51	22	—
Test	6.10	0.09	0.10	1.65	4.45	225	—
JBDS	6.10	0.06	0.06	1.72	4.37	63	—
Test	9.93	0.16	0.17	2.68	7.25	378	—
JBDS	9.93	0.17	0.17	2.81	7.11	339	—
Test	14.39	0.27	0.27	3.95	10.44	616	—
JBDS	14.39	0.30	0.30	4.07	10.32	509	—
Test	16.36	0.31	0.31	4.49	11.87	715	—
JBDS	16.36	0.35	0.35	4.64	11.72	584	—

Note: 1 in. = 25.4 mm; 1 kip = 4.45 kN.

Structural Analysis Program JBDL

A structural analysis program JBDL (Jointless Bridge Deck Link) was developed by the first author[17] using the conventional beam element. Each element has two end nodes, each with three degrees of freedom (in horizontal, vertical and rotational directions). In the computer model, the bridge is divided into several segments and each segment is represented by an element. The section properties of each element are defined with respect to its own neutral axis.

During the analysis, the computer program checks for cracking of the link slab element. If the program detects cracking of the link slab, the program repeats the analysis with the new moment of inertia and area for the cracked section of the link slab and estimates the surface crack width of the link slab using the crack criteria specified in the AASHTO Specifications.[19] The program can analyze the effects of applied loads, creep, shrinkage and temperature differentials. More detailed information on the program can be found in Ref. 17.

Steel Bridge — Each span of the steel bridge was analyzed first as a simply-supported composite girder by a finite element program, JBDS, developed by El-Safty[8] to investigate the behavior of the specimen under increasing load. For loads up to 40 percent of the ultimate load, the analytical

results indicated that the specimen behaved elastically and no yielding of the steel beams was predicted.

For the HRRH case, the measured strains at the bottom of the section located at 13 ft (4.01 m) from the outer reaction of each span were predicted with reasonable accuracy by the JBDS program,[8] as shown in Table 3. The predicted outer and inner reactions also compared closely with the measured data.

For other test cases with support configurations RHHR, RRRR and RHRH, similar responses to the applied loads were obtained. It is concluded that the program JBDS is reliable for analyzing the steel bridge as a simply-supported structure because the effect of the stiffness of the link slab is negligible.

The program JBDL was then used to analyze the stresses and surface crack widths in the link slab. As observed in the test of the specimen, the program predicted tension at the top surface and compression at the bottom surface of the link slab. The predicted reinforcing bar stresses compared reasonably well with the measured data as shown in Table 4. The ratio of the predicted to the measured reinforcing bar stress ranges from 0.97 to 1.16. The ratio of the predicted crack width to the measured crack width lies between 1.06 and 1.27. The results of simplified method are more conservative than the test data as shown in Table 4.

Concrete Bridge — The same type of analysis as for the steel bridge was also applied to the concrete bridge. By using the JBDS program, each span of the concrete bridge was analyzed as a simply-supported structure. With a load of 40 percent of the ultimate load, the results of analyses indicated that cracking initiated in the concrete beam. The program then calculated the effective areas and moments of inertia of the cracked elements and continued with the analysis.

For the HRRH case, the measured strains in the lower level reinforcement of the east concrete beam at a section 14 ft (4.27 m) from the outer reaction were predicted reasonably well by the program, as shown in Table 3. It is noted that the exterior and interior reactions were closely predicted by the program.

The stresses in the link slab were then predicted by analyzing the struc-

Table 4. Comparison of test results with predictions by JBDL program and simplified method.

Test specimen	Results	Support configuration	Applied load *P* (kips)	Midspan deflection (in.)	Exterior reaction (kips)	Interior reaction (kips)	Link slab reinforcing bar stress (ksi)	Link slab crack width (in.)
Steel bridge	Test	RHHR	3.85	0.06	0.83	3.02	4.35	0.002
	JBDL		3.85	0.05	0.99	2.86	0.00	0.000
	Simplified		3.85	0.05	1.10	2.74	0.00	0.000
	Test	RHHR	12.05	0.21	3.26	8.79	12.73	0.010
	JBDL		12.05	0.15	3.27	8.78	15.75	0.014
	Simplified		12.05	0.16	3.45	8.59	19.58	0.016
	Test	RHHR	17.43	0.32	4.95	12.48	18.65	0.015
	JBDL		17.43	0.22	4.77	12.66	18.91	0.016
	Simplified		17.43	0.23	4.99	12.43	25.81	0.021
	Test	RHRH	17.43	0.31	4.67	12.76	16.25	—
	JBDL		17.43	0.22	4.77	12.66	18.91	0.016
	Simplified		17.43	0.23	4.99	12.43	25.81	0.021
	Test	HRRH	17.43	0.33	4.94	12.49	19.47	—
	JBDL		17.43	0.22	4.77	12.66	18.91	0.016
	Simplified		17.43	0.23	4.99	12.43	25.81	0.021
Concrete bridge	Test	RHHR	2.24	0.03	0.55	1.69	1.09	0.000
	JBDL		2.24	0.02	0.58	1.66	0.00	0.000
	Simplified		2.24	0.05	0.66	1.58	0.00	0.000
	Test	RHHR	10.24	0.19	2.65	7.59	10.98	0.008
	JBDL		10.24	0.16	2.73	7.51	18.64	0.016
	Simplified		10.24	0.24	3.02	7.22	30.74	0.025
	Test	RHHR	16.30	0.32	4.35	11.95	18.89	0.020
	JBDL		16.30	0.33	4.37	11.93	25.55	0.022
	Simplified		16.30	0.38	4.80	11.49	49.30	0.039
	Test	RHRH	16.30	0.32	4.40	11.90	17.94	0.010
	JBDL		16.30	0.33	4.37	11.93	35.55	0.022
	Simplified		16.30	0.38	4.80	11.49	49.30	0.039
	Test	HRRH	16.30	0.31	4.39	11.91	19.00	0.012
	JBDL		16.30	0.33	4.37	11.93	25.55	0.022
	Simplified		16.30	0.38	4.80	11.49	49.30	0.039

Note: 1 in. = 25.4 mm; 1 kip = 4.45 kN; 1 ksi = 6.895 MPa.

ture using the JBDL program. The program predicted tension at the top surface and compression at the bottom surface of the link slab as observed in the tests. The reinforcing bar stresses as predicted by JBDL compared reasonably well with the experimental data presented in Table 4.

The ratio of the predicted to the measured reinforcing bar stress ranges between 1.35 and 1.69. The predicted crack widths on the top surface of the link slab are larger than the measured values. The ratio of the predicted to the measured crack width ranges between 1.10 and 1.45. Again, the simplified method is shown to be more conservative.

PROPOSED DESIGN METHOD

Currently, there is no formal design procedure for jointless bridge decks with debonded link slabs. Based on the results of available analytical studies and the test program presented herein, a simple design method can be developed as follows:

1. Each span of a bridge with a jointless bridge deck may be designed independently as a simply-supported span using standard design procedures without considering the effect of the link slab because the stiffness of the link slab is much smaller when compared to that of the composite girders.

2. Provide debonding of 5 percent of each girder span for the link slab to further reduce its stiffness. El-Safty's studies[8] indicated that the load-deflection behavior of jointless bridge decks supported by simple-span girders is not affected by debonding up to 5 percent of the span length.

3. Determine the maximum end rotations of the girders as simply-supported under service load and impose the end rotations to the ends of the link slab. Determine the moment M_a in the link slab due to the imposed end rotations, using the gross section property of the link slab (which is conservative because the link slab will develop small cracks causing a reduction in its stiffness). Design the reinforcement for the link slab using a conservative working stress such as 40 percent of the yield strength of the reinforcing bar.

Table 5. Preliminary design table for link slab with compressive strength f'_c = 3000 psi; modulus of flexure f_r = 400 psi; modular ratio n = 9; ratio of reinforcement depth to link slab thickness γ = 0.8.

	Stress in link slab reinforcement, f_s (ksi)					
M_{cr}/M_a	ρ = 0.005	ρ = 0.010	ρ = 0.015	ρ = 0.020	ρ = 0.025	ρ = 0.030
0.9		14.46	10.27	8.19	6.98	6.18
0.8		16.24	11.55	9.21	7.83	6.95
0.7		18.56	13.20	10.53	8.96	7.93
0.6		19.57	15.42	12.27	10.46	9.25
0.5		20.57	18.49	14.74	12.55	11.17
0.4			23.10	18.43	15.66	13.89
0.3					20.88	18.56

Note: 1 ksi = 6.895 MPa.

Table 6. Preliminary design table for link slab with compressive strength f'_c = 3000 psi; modulus of flexure f_r = 400 psi; modular ratio n = 9; ratio of reinforcement depth to link slab thickness γ = 0.6.

	Stress in link slab reinforcement, f_s (ksi)					
M_{cr}/M_a	ρ = 0.005	ρ = 0.010	ρ = 0.015	ρ = 0.020	ρ = 0.025	ρ = 0.030
0.9			18.26	14.56	12.38	10.98
0.8			20.54	16.37	13.93	12.35
0.7			23.47	18.72	15.92	14.12
0.6				21.84	18.57	16.47
0.5					22.29	19.76
0.4						
0.3						

Note: 1 ksi = 6.895 MPa.

Table 7. Preliminary design table for link slab with compressive strength f'_c = 4000 psi; modulus of flexure f_r = 480 psi; modular ratio n = 8; ratio of reinforcement depth to link slab thickness γ = 0.8.

	Stress in link slab reinforcement, f_s (ksi)					
M_{cr}/M_a	ρ = 0.005	ρ = 0.010	ρ = 0.015	ρ = 0.020	ρ = 0.025	ρ = 0.030
0.9		16.40	11.57	9.15	7.72	6.78
0.8		18.45	13.01	10.30	8.68	7.63
0.7		21.09	14.87	11.77	9.93	8.72
0.6			17.35	13.73	11.58	10.18
0.5			20.82	16.47	13.90	12.21
0.4				20.59	17.37	15.26
0.3					23.16	20.35

Note: 1 ksi = 6.895 MPa.

Table 8. Preliminary design table for link slab with compressive strength f'_c = 4000 psi; modulus of flexure f_r = 480 psi; modular ratio n = 8; ratio of reinforcement depth to link slab thickness γ = 0.6.

	Stress in link slab reinforcement, f_s (ksi)					
M_{cr}/M_a	ρ = 0.005	ρ = 0.010	ρ = 0.015	ρ = 0.020	ρ = 0.025	ρ = 0.030
0.9			20.56	16.27	13.72	12.06
0.8			23.13	18.30	15.44	13.57
0.7				20.92	17.64	15.51
0.6					20.59	18.09
0.5						21.71
0.4						
0.3						

Note: 1 ksi = 6.895 MPa.

Table 9. Preliminary design table for link slab with compressive strength f'_c = 5000 psi; modulus of flexure f_r = 540 psi; modular ratio n = 7; ratio of reinforcement depth to link slab thickness γ = 0.8.

	Stress in link slab reinforcement, f_s (ksi)					
M_{cr}/M_a	ρ = 0.005	ρ = 0.010	ρ = 0.015	ρ = 0.020	ρ = 0.025	ρ = 0.030
0.9		18.11	12.71	10.00	8.39	7.33
0.8		20.37	14.30	11.26	9.44	8.25
0.7		23.28	16.34	12.86	10.79	9.43
0.6			19.06	15.01	12.59	11.00
0.5			22.87	18.01	15.11	13.20
0.4				22.51	18.88	16.50
0.3						22.00

Note: 1 ksi = 6.895 MPa.

Table 10. Preliminary design table for link slab with compressive strength f'_c = 5000 psi; modulus of flexure f_r = 540 psi; modular ratio n = 7; ratio of reinforcement depth to link slab thickness γ = 0.6.

	Stress in link slab reinforcement, f_s (ksi)					
M_{cr}/M_a	ρ = 0.005	ρ = 0.010	ρ = 0.015	ρ = 0.020	ρ = 0.025	ρ = 0.030
0.9			22.59	17.79	14.92	13.04
0.8				20.01	16.79	14.67
0.7				22.87	19.18	16.76
0.6					22.38	19.56
0.5						23.47
0.4						
0.3						

Note: 1 ksi = 6.895 MPa.

4. Use the crack control criteria of the AASHTO Specifications[19] to limit the crack width at the surface of the link slab to 0.013 in. (0.33 mm) for exterior exposure. The AASHTO crack width control criterion is given as:

$$z \leq f_s(d_c A)^{1/3}$$

in which $z \leq 143$ kips/in. (25 MN/m). The term f_s (steel stress in reinforcing bars) can be obtained from the preliminary Design Tables 5 through 10, which are based on the equations summarized in Fig. 4.

To illustrate the above design procedure, three design examples are given in the Appendix.

CONCLUSIONS

Based on the results of this investigation, the following conclusions may be drawn:

1. Within the elastic range, the measured deflections, the strains in the girders, and the strains in the link slab reinforcement were not affected by the variations of support conditions (hinge vs. roller) at the exterior and interior supports.

2. Because the stiffness of the link slab was much smaller than that of the composite girders, the continuity introduced by the link slab was negligible. Therefore, each of the two composite girders behaved like a simply-supported girder.

3. With the girders being treated as simply-supported, the predicted girder deflections compared closely with the measured deflections of the test specimens.

4. Under test loading, the measured strain variation through the depth of the link slab indicated that the link slab was under bending rather than in direct tension. The link slab failed in bending with concrete cracking at its top face and concrete crushing at its bottom face.

5. Both the computer solution and the simplified method of analysis overestimated slightly the reinforcement stress and crack width in the link slab. The simplified method of analysis was more conservative than the computer solution.

6. Because the link slab introduces negligible continuity to a multispan bridge, the girder for each bridge span can be designed independently as a simply-supported structure. The adjacent spans can then be connected by link slabs with partial debonding.

7. The link slab can easily be designed by the simple method proposed herein to provide sufficient reinforcement for crack control.

8. As demonstrated by this investigation, the concept of replacing standard bridge deck joints by link slabs to form a jointless bridge deck is entirely feasible. Such an approach would result in significant savings in the cost of construction and maintenance of bridge decks.

RECOMMENDATIONS AND FUTURE RESEARCH

The concept of a link slab with partial debonding from adjacent girders should be readily applicable to typical multispan highway bridge decks to reduce the number of standard expansion joints. It is recommended that for bridges of up to four spans, all the interior joints may be replaced by link slabs so that up to 60 percent of the expansion joints could be eliminated. The concept can be used in both new bridge construction and in the rehabilitation of deteriorated bridge decks.

Because cracking of the link slab is expected to occur under normal service load conditions, it is recommended that epoxy coated reinforcing bars be used in the link slab in order to minimize the potential for reinforcement corrosion. In lieu of epoxy coated bars, non-metallic reinforcement such as carbon fiber reinforced polymer (FRP) bars can also be used. To control cracking in the link slab, a shallow transverse saw cut may be made at the center of the link slab to localize the crack. The saw cut may be filled with a hot-poured sealant to improve its serviceability.

Future research should include a performance evaluation of actual field installations of link slabs. In this regard, a demonstration bridge involving deck replacement has been designed by the North Carolina Department of Transportation utilizing the concept of link slabs. The project is under construction and the link slab will be instrumented for long-term evaluation.

Additional research should also include more detailed theoretical and experimental studies of the effects of temperature, creep, and shrinkage on the behavior of link slabs so that the design of bridge decks with link slabs can be optimized.

ACKNOWLEDGMENT

The research described in this paper was sponsored by the North Carolina Department of Transportation and the Federal Highway Administration, and administered by the Center for Transportation Engineering Studies at North Carolina State University at Raleigh.

The authors are indebted to the Technical Advisory Committee composed of J. L. Smith (chairman), J. R. Wilder, R. W. Reaves, of the North Carolina Department of Transportation and P. A. Simon of the Federal Highway Administration, who provided continuing guidance for the research project.

The authors also extend special thanks to a group of former and current graduate students at North Carolina State University including Dena Guth, Adel El-Safty, Randall Hillmann, Carl Jerrett, and Eggert Valmundsson who gave invaluable help in casting the test specimens and in conducting the tests at the various stages of the project.

Finally, the authors wish to express their gratitude to the PCI JOURNAL reviewers for their suggestions in improving the clarity of the paper.

REFERENCES

1. Burke, M. P., Jr., "The Design of Integral Bridges," *Concrete International*, V. 15, No. 6, June 1993, pp. 37-42.
2. Burke, M. P., Jr., "Semi-Integral Bridges: Movements and Forces," Transportation Research Record 1460, December 1994, pp. 1-7.
3. Burke, M. P., Jr., "Integral Bridges: Attributes and Limitations," Paper presented at ACI National Concrete Engineering Conference, Chicago, IL, March 1992.
4. Kamel, M. R., Benak, J. V., Tadros, M. K., and Jamshidi, M., "Prestressed Concrete Piles in Jointless Bridges," PCI JOURNAL, V. 41, No. 2, March-April 1996, pp. 56-67.
5. Wasserman, E. P., "Jointless Bridge Decks," *AISC Engineering Journal*, V. 24, No. 3, Third Quarter 1987, pp. 93-100.
6. Loveall, C. L., "Jointless Bridge Decks," *Civil Engineering*, V. 55, No. 11, November 1985, pp. 64-67.
7. Oesterle, R. G., Glikin, J. D., and Larson, S. C., "Design of Precast, Prestressed Bridge Girder Made Continuous," NCHRP Report 322, National Research Council, Washington, D.C., November 1989, 108 pp.
8. El-Safty, A. K., "Analysis of Jointless Bridge Decks with Partially Debonded Simple Span Beams," Ph.D. Dissertation, North Carolina State University, Raleigh, NC, 1994.
9. Demartini, C. J., and Heywood, R. J., "Repair of the Southern Approach to the Story Bridge by Elimination of the Contraction Joints," *Austroads Conference*, Brisbane, Australia, 1991, pp. 357-370.
10. Underwood, R. T., "The Hume (Melbourne-Sydney) Freeway in the State of Victoria, Australia," Proceedings of Institution of Civil Engineers (London), Part 1, No. 84, April 1988, pp. 265-290.
11. Bassi, K. G., Discussion of "The Hume (Melbourne-Sydney) Freeway in the State of Victoria, Australia," Proceedings of Institution of Civil Engineers (London), Part 1, No. 86, April 1989, p. 435.
12. Zuk, W., "Jointless Bridges," Research Report No. FHWA/VA-81/48, Virginia Highway and Transportation Research Council, Charlottesville, VA, June 1981, 44 pp.
13. Gastal, F., and Zia, P., "Analysis of Bridge Beams with Jointless Decks," Proceedings of IASBE Symposium, Lisbon, Portugal, September 1989, pp. 555-560.
14. Gastal, F., "Instantaneous and Time-Dependent Response and Strength of Jointless Bridge Beams," Ph.D. Dissertation, North Carolina State University, Raleigh, NC, 1986.
15. Richardson, D. R., "Simplified Design Procedures for the Removal of Expansion Joints from Bridges Using Partial Debonded Continuous Decks," MSCE Thesis, North Carolina State University, Raleigh, NC, 1989.
16. Zia, P., Caner, A., and El-Safty, A. K., "Jointless Bridge Decks," Research Report No. FHWA/NC/95-006, Center for Transportation Engineering Studies, North Carolina State University, Raleigh, NC, September 1995.
17. Caner, A., "Analysis and Design of Jointless Bridge Decks Supported by Simple-Span Girders," Ph.D. Dissertation, North Carolina State University, Raleigh, NC, 1996.
18. Tall, L. (Editor), *Structural Steel Design*, Second Edition, Ronald Press, New York, NY, 1974, p. 476.
19. AASHTO Highway Subcommittee on Bridges and Structures, *Standard Specifications for Highway Bridges*, Sixteenth Edition, American Association of State Highway and Transportation Officials, Washington, D.C., 1996.
20. Gergely, P., and Lutz, L. A., "Maximum Crack Width in Reinforced Concrete Flexural Members," *Causes, Mechanism, and Control of Cracking in Concrete*, SP-20, American Concrete Institute, Farmington Hills, MI, 1968, pp. 87-117.
21. *PCI Design Handbook*, Fourth Edition, Precast/Prestressed Concrete Institute, Chicago, IL, 1992.

APPENDIX — DESIGN EXAMPLES

EXAMPLE 1

Design the link slab for a two-lane bridge of four equal spans of 73 ft (22.3 m) each. The distance between the ends of two adjacent girders is 2 in. (50 mm). The overall girder length is 72 ft 10 in. (22.2 m). The center-to-center width of bearings of each simply-supported girder is 71.5 ft (21.8 m). The cross section of the bridge and its longitudinal section are shown in Fig. A1.

Each of the AASHTO Type III girders is prestressed with 28 low-relaxation strands of 0.5 in. (13 mm) diameter. The 8 in. (200 mm) thick deck includes 3 in. (75 mm) thick prestressed concrete stay-in-place slab and 5 in. (125 mm) cast-in-place concrete topping. The deck is reinforced with #6 transverse bars at 7 in. (175 mm) on centers and #4 longitudinal bars at 9 in. (225 mm) on centers. The concrete cover over the transverse bars is 2.5 in. (63 mm).

The specified 28-day compressive strength of concrete is 7500 psi (52 MPa) for the girder and 4500 psi (31 MPa) for the deck. Use E_c = 4950 ksi (34.2 GPa) for the girder and E_c = 3825 ksi (26.4 GPa) for the deck. Assume the flexural modulus f_r = 500 psi (3.5 MPa) for the deck concrete. Use AASHTO HS20-44 lane loading.

Solution — Allowing 5 percent debonding at each end of girder, the length of the link slab for design would be: $L = 2 \times 0.05 \times 73 \times 12 = 87.6$ in. (2190 mm).

Treat each composite girder as simply supported. Due to the difference in the values of E_c for the girder and the deck, use the transformed section of the deck to compute the moment of inertia of the composite girder, which is I_g = 349,400 in.^{4} (14,540,000 cm^4).

Apply AASHTO HS20-44 lane loading including impact to the composite girder with a design span of 71.5 ft (21.8 m) and compute the end rotation of the girder at support $\theta = 0.00147$ radians.

With a link slab width = 6.92 ft (2.11 m) and thickness = 8 in. (200 mm), the moment of inertia of the link slab I_d = 3540 in.^{4} (147,500 cm^4). Apply an end rotation of $\theta = 0.00147$ radians at both ends of the link slab with a design span L = 87.6 in. (2190 mm). The negative moment induced in the link slab due to the applied end rotation is computed as:

$$M_a = 2E_cI_d\theta/L = 37.8 \text{ ft-kips } (51.7 \text{ kN-m})$$

The cracking moment of the link slab $M_{cr} = f_rI/y = 500 \times 3540/4 = 36.9$ ft-kips (50.5 kN-m). So, $M_{cr}/M_a = 0.98$. Thus, the induced negative moment in the link slab exceeds its cracking moment by about 2 percent and hairline cracks can be expected on the top surface of the link slab.

To design the reinforcement for the link slab, try #6 bars at 8 in. (200 mm) on centers and allow 2.5 in. (63 mm) for concrete cover from the top face of the link slab. Then the

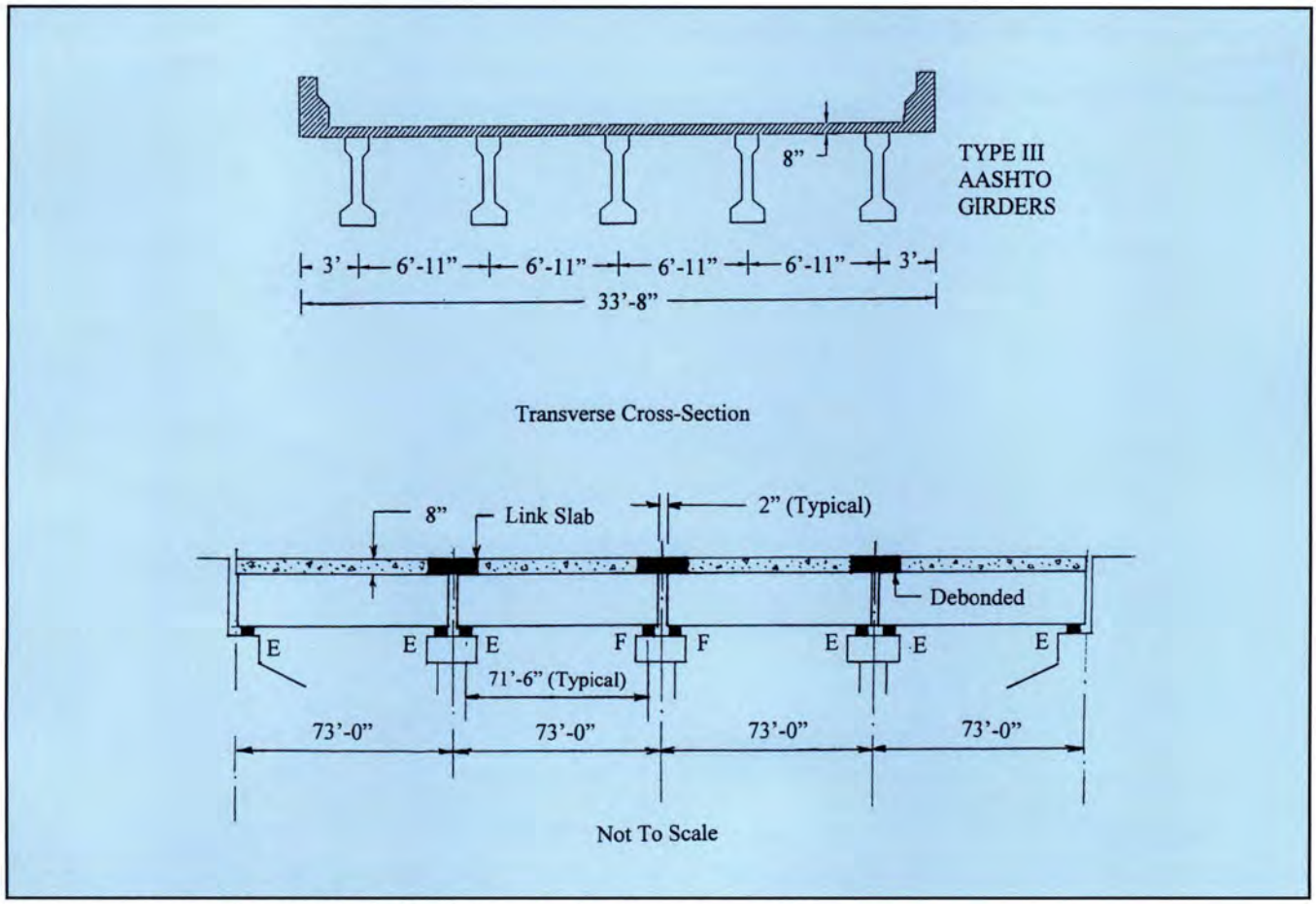

Fig. A1. Cross-sectional views of bridge for design examples. **Note:** 1 in. = 25.4 mm.

effective depth d = 5.5 in. (138 mm). Therefore, the reinforcement ratio $\rho = 0.44/8 \times 5.5 = 0.01$.

Use Eq. (9) in Fig. 4 to determine the steel stress due to M_a. Because $\rho = 0.01$, $n = 7.84$, and $\gamma = 5.5/8 = 0.6875$, from Eq. (9) one obtains f_s = 20,250 psi (140 MPa).

Check the crack width control criterion in terms of the z-value. Because d_c = 5.5 in. (138 mm) and $A = 8 \times 2.5 \times 2 = 40$ sq in. (250 cm^2):

$z = f_s(d_c A)^{1/3} = 20.25(5.5 \times 40)^{1/3}$
= 122 kips/in. (21.4 MN/m) < 143 kips/in. (25 MN/m)

Therefore, the crack width control criterion is satisfied and #6 bars at 8 in. (200 mm) on centers is acceptable.

EXAMPLE 2

Determine the steel stress in the above link slab due to a temperature differential in the deck-girder system. Assume that the temperature drop at the top of the deck is 50°F (27.8°C) and at the bottom of the girder is 20°F (11.1°C).

Solution — The temperature variation represents a differential of 30°F (16.7°C) and the deck-girder system will deflect downward due to this temperature differential. Again, each composite girder can be treated as simply supported. The end rotation of the girder consistent with its vertical deflection can be calculated by any conventional method and is found to be $\theta = 0.00158$ radians.

As in Example 1, the negative moment induced in the link slab would be M_a = 40.6 ft-kips (55.5 kN-m). Then $M_{cr}/M_a = 0.91$. As before, using Eq. (9) of Fig. 4, one obtains f_s = 21,810 psi (150.5 MPa).

Similarly, z = 131 kips/in. (22.9 MN/m) < 143 kips/in. (25 MN-m).

Therefore, the design is acceptable.

EXAMPLE 3

Determine the steel stress in the above link slab due to the effects of shrinkage and creep of concrete. Based on the data given in the PCI Design Handbook,[21] assume that the final shrinkage and creep strains in the deck are 0.000448 and 0.000073, respectively, and that the final shrinkage and creep strains in the girder are 0.000357 and 0.000454, respectively.

Solution — Again as before, each composite girder is treated as simply supported and subjected to differential shrinkage and creep strains between the girder and the deck. Because the girder will sustain a much larger strain than the deck, the composite girder will deflect upward and produce a negative end rotation θ = 0.0029 radians. Imposing this same end rotation at each end of the link slab will induce a positive moment in the link slab, which is found to be M_a = 74 ft-kips (100 kN-m).

Therefore, $M_{cr}/M_a = 0.5$.

Using Eq. (9) of Fig. 4, f_s = 39,690 psi (274 MPa).

Similarly, z = 238 kips/in. (41.6 MN/m) > 143 kips/in. (25 MN/m).

Therefore, the crack control criterion is exceeded. A revised design using #7 bars at 6 in. (150 mm) on centers would result in f_s = 22,730 psi (157 MPa) and z = 125 kips/in. (21.8 MN/m) < 143 kips/in. (25 MN/m). It is noted that the effects of shrinkage and creep are to induce a positive moment in the link slab and cracking would occur on the bottom face of the link slab. So the reinforcement should be placed near the bottom of the link slab.